Analysis and minimization of dislocation interactions with atomistic/continuum interfaces

2006 Modelling Simul. Mater. Sci. Eng. 14 497

(http://iopscience.iop.org/0965-0393/14/3/011)

INSTITUTE OF PHYSICS PUBLISHING MODELLING AND SIMULATION IN MATERIALS SCIENCE AND ENGINEERING

Modelling Simul. Mater. Sci. Eng. **14** (2006) 497–514 doi:10.1088/0965-0393/14/3/011

Analysis and minimization of dislocation interactions with atomistic/continuum interfaces

M Dewald and W A Curtin

Division of Engineering, Brown University, Providence, RI 02906, USA

Received 9 October 2005
Published 10 April 2006
Online at stacks.iop.org/MSMSE/14/497

Abstract

Spurious forces are shown to arise when dislocations interact with atom/continuum interfaces in some classes of multiscale models due to the use of linear elasticity in continuum descriptions of the material deformations and/or the singular dislocation fields. For Al, such forces can reach 500 MPa for dislocations within a few Angstroms of the interface and can remain significant at distances of ∼20 Å on the atomistic side and ∼15 Å on the continuum side of the interface, inhibiting the creation of truly seamless coupling. Replacement of the continuum representation of the dislocation displacement fields by a 'template' of the full atomistic displacement fields within a radius of $R_{\text{core}} =$ 50 Å is shown to significantly reduce the magnitude and range of the spurious forces. Implementation of the template method permits dislocations to approach within less than 10 Å of the interface from both atomistic and continuum sides, permitting higher accuracy in the multiscale simulations as well as reduced size of the atomistic region.

(Some figures in this article are in colour only in the electronic version)

1. Introduction

Macroscopic mechanical behaviour in solids such as plasticity and fracture is inherently influenced by atomic scale processes. Atomistic models can address these processes (dislocation nucleation, mobility, crack formation and propagation, etc) but are limited in size because of the many degrees of freedom necessary when treating each individual atom. Continuum models can use phenomenological descriptions of atomic scale behaviour, but these rules might not be simple or even be known. For example, dislocation core interactions with other material defects are generally not captured accurately from continuum models, and these short range interactions can effect defect position and motion over long ranges, thus influencing large scale behaviour. Therefore, multiscale models have been developed that capture atomistic phenomena at one scale and important mesoscale phenomena at larger scales, thus bridging the multiple length scales that govern material behaviour. In these methods a critical region or regions, much smaller than the overall computational domain, is defined using atomic level

descriptions capable of producing appropriate behaviour at the nanoscale. Most multiscale models use empirical potentials [1–11], which are generally satisfactory in describing a wide range of atomistic phenomena and have been used extensively in most full molecular static or dynamic investigations to date. Quantum mechanical calculations have also been performed within these methods [13, 14] but are only computationally tractable in very limited circumstances. Outside of the atomistic region, where strain fields are smoothly varying, continuum mechanics is used to describe the material deformation behaviour over larger length scales. Many multiscale methods restrict non-linear defect descriptions to small pre-defined atomistic regions [1–4, 13, 14], while a subset of these atomistic/continuum coupled techniques allow material defects to exist and travel throughout the entire computational model [5–11]. Plastic response of materials is affected by the long range interactions of dislocations. Therefore, methods that permit the range of dislocations to span over large computational cell sizes are particularly useful in studying mechanical behaviour.

The quasicontinuum (QC) [5–7] and the coupled atomistic discrete dislocation (CADD) methods [8–11] are two models that employ atomistics where necessary as well as allow for long range dislocation interactions. The QC method requires full atomic resolution of any non-linearity or defect in the system. Thus, dislocations carry their full non-linear, non-local atomistic core as they move through space through the implementation of an automatic adaption scheme. In contrast, CADD considers a fixed atomistic domain but allows a dislocation to exist as either a fully atomistic entity in that domain or as a continuum entity (line defect in an elastic medium) in the surrounding continuum domain. A distinctive feature of CADD is that a dislocation can pass nearly seamlessly between the atomistic and continuum domains so that the major approximation in the CADD method is the use of the continuum dislocation representation itself. This approximation is almost a tenet of multiscale models—far from some critical region requiring full atomistic treatment the atomistic details (e.g. dislocation core structure of any particular dislocation) are not important and need not be carried along explicitly in the computation. Therefore, the long-range interactions of a large number of dislocations with specific defects (e.g. dislocation pile-ups with grain boundaries, dislocation density surrounding crack tip regions, etc) as well as short range interactions of these defects with dislocation cores can be studied without the use of any phenomenological rules. This is distinctive from standard discrete dislocation models that rely solely on continuum descriptions and thus cannot explicitly capture atomic scale phenomena.

In the QC and CADD methodologies as well as in other atom/continuum coupling methods, dislocation core structures can possibly reside near an atomistic/continuum interface [1–14]. In the standard QC method, so-called ‘ghost forces’ lead to spurious displacements at the atom/continuum interface and these distortions can interact with the dislocation to produce spurious forces. Similar effects can occur in other coupled methods [1–4], depending on how the continuum deformations are handled. Large deformation gradients near atomistic/continuum interfaces can produce spurious forces within the atom/continuum coupling method employed in the CADD method [12], and dislocation core structures do produce such deformations. Rao *et al* have already demonstrated, within the Lattice Green’s Function method, that interface forces are significant when an atomistic region is smaller than 3.5–4 times the dislocation core width [13, 14]. If these spurious forces are considerable then a dislocation can experience incorrect driving forces and become artificially trapped, repelled or distorted near the atomistic/continuum interface region. Not only will the dislocation positions be inaccurate, but the resulting stress state on other defects and dislocations could also produce incorrect behaviour. Thus, it is desirable to understand and minimize spurious forces occurring in any computational scheme and thereby minimize the region of space that cannot support dislocation defects to as small a region as possible.

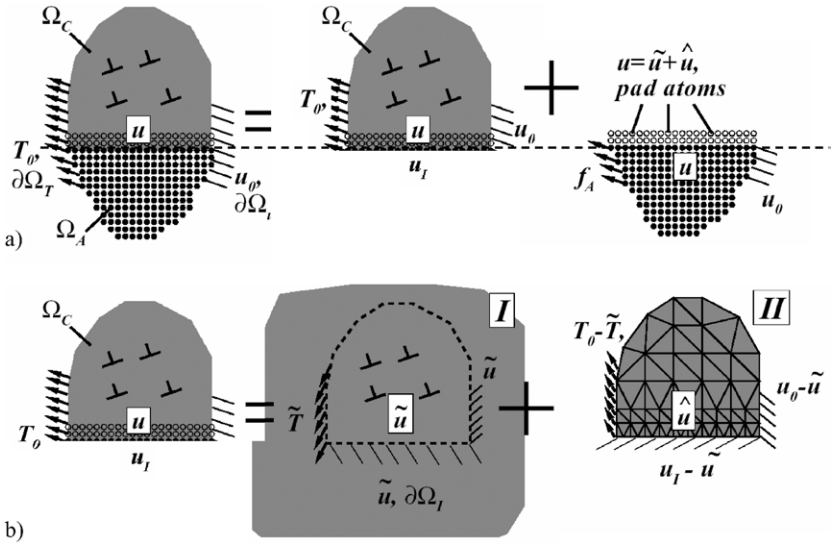

Figure 1. Schematic illustration of the CADD solution procedure. (*a*) The total problem is divided into a continuum and atomistic domain coupled together by appropriate boundary conditions along the interface. (*b*) The continuum domain is split into two subproblems; the first treats all continuum dislocations as line defects in an infinite medium while the second consists of a linear elastic FEM problem subject to the true boundary conditions minus the fields that the first problem would place on the boundary.

With the above perspective, the purpose of this paper is two-fold. First, the error in dislocation driving forces for dislocations near the atomistic/continuum interface employed in the CADD method is quantified. Second, an improved, efficient method that permits dislocations to move closer to the atomistic/continuum interface from either side of the interface while maintaining high accuracy on the forces and deformations is formulated and evaluated. The method can also be used to lessen the interaction of atomistic dislocations with atom/continuum interfaces in other coupled methods [1–4] and thus has a generality that goes beyond its specific application within the CADD model.

The rest of this paper is organized as follows. In section 2 we briefly review the CADD coupling methodology. In section 3, we quantitatively analyse the spurious forces on dislocations near the atom/continuum interface in the CADD model, for FCC Al. In section 4 we introduce a 'template' method to significantly reduce the spurious forces in magnitude and/or range, and discuss the implications of the method for modelling within CADD. Section 5 summarizes our main results and their impact on multiscale modelling methods.

2. CADD methodology

CADD solves a boundary value problem consisting of tractions T_0 and/or displacements u_0 specified on a domain containing atomistic region(s) and continuum region(s) by dividing it into two problems, one for each domain (figure 1(*a*)) and coupling them by appropriate boundary conditions along the interface [8–11]. The atomistic problem is treated by interatomic potentials; any atomic scale defects (dislocations, grain boundaries, cracks, voids) can exist and interact naturally inside this domain without the use of any phenomenological rules. The continuum problem is solved using the discrete dislocation methodology of van der Giessen

and Needleman [15], which involves two subproblems (figure 1(*b*)). The first continuum subproblem consists of the dislocation line defects embedded in an infinite elastic medium; the total stress $\tilde{\sigma}$ and displacement $\tilde{\boldsymbol{u}}$ fields are computed by summation of the known analytic dislocation fields [8–11]. This analytic solution has corresponding tractions $\tilde{T}$ and displacements $\tilde{\boldsymbol{u}}$ along the true continuum boundary that do not solve the boundary value problem. The second continuum subproblem consists of a linear elastic problem in the continuum region subject to the true applied boundary conditions minus the analytic fields, $\hat{T} = T_0 - T$, $\hat{\boldsymbol{u}} = u_0 - \tilde{\boldsymbol{u}}$. The finite element method is used to solve for the smooth fields of the second continuum subproblem, which has no singular fields due to the dislocations. Superposition of the fields in the two continuum subproblems yields the solution for the total fields that satisfies equilibrium and the correct traction and displacement boundary conditions on the continuum region. This solution method is valid if the material behaviour is linearly elastic; it also requires linear behaviour in the associated atomistic region near the atom/continuum interface, as discussed below. The Peach–Koehler (P–K) driving force $\boldsymbol{p}^i$ on the ith continuum dislocation is then calculated using the full continuum fields as

$$\boldsymbol{p}^i = (\boldsymbol{m}^i)^T \left[\hat{\sigma} + \sum_{j \neq i}^{\sim} \tilde{\sigma}_j \right] (\boldsymbol{b}^i), \tag{1}$$

where $\boldsymbol{m}^i$ is the slip plane normal of dislocation i and $\boldsymbol{b}^i$ is the Burgers' vector. The boundary conditions along the interface between the atomistic and continuum regions used to couple the two regions are as follows. The continuum problem uses the atomistic positions along the atom/continuum interface as a displacement boundary condition for any incremental solution; this ensures continuity of displacements across the interface. Special 'pad atoms' that overlap the continuum region are added to the atomistic problem to serve as a boundary layer of atoms that provide the proper atomistic forces onto the real atoms. The positions of the pad atoms are calculated from the continuum fields as $\boldsymbol{u}_p = \hat{\boldsymbol{u}} + \tilde{\boldsymbol{u}}$, using the finite element interpolation functions to convey the proper displacement field $\hat{\boldsymbol{u}}$ to each pad atom. The coupled deformation of the atomistic and continuum regions, including the continuum dislocation degrees of freedom, is then solved using an iterative scheme with the conjugate gradient method.

During the course of reaching equilibrium under the applied loading, dislocations existing in the atomistic or continuum region may have equilibrium positions in the other region. To attain the proper equilibrium state, such dislocations must be converted from one description to the other, and moved from one region to the other, by 'passing' across the atomistic/continuum interface. 'Passing' a dislocation first requires detection of the dislocation at some specified distance from the interface. In the atomistic region, the dislocation consists of a special atomic arrangement composing the dislocation core, which must thus be identified. In CADD, detection of dislocations within the atomistic region is accomplished by creating a 'detection band' of triangular elements defined by neighbouring atoms in their reference configuration and located at a distance R_{DB} from the interface. The Lagrangian strain within each detection band element is continuously computed and compared against a library of strain fields for each possible dislocation slip system within the crystal. If the strain field in an element matches that for a slip system, within some tolerance, a dislocation core with known Burgers' vector and slip plane is then known to reside in that element. To pass the dislocation at the passing distance $R_{A\to C}$, with $R_{A\to C} = R_{DB}$ in the usual case, the dislocation core position is artificially moved along its slip plane into the continuum region to a distance $R_{C\to A} + \Delta$ from the interface as a continuum entity ($\Delta \sim 2$ Å). The original displacement field in the atomistic regime is annihilated by adding the displacement field of a dislocation with opposite Burgers vector at the

centre of the band element and then relaxing the atoms. In the continuum region, the discrete dislocation always has a specific position and so is trivially detected when it reaches a passing distance $R_{C\to A}$ from the interface. At that point, the continuum dislocation is removed from the continuum and an atomistic dislocation core is added in the atomistic region at distance $R_{A\to C}+\Delta$ along the slip plane from the interface. Once in the atomistic regime, the dislocation moves according to the atomic-level forces. A continuum 'ghost dislocation' is also placed along the slip plane somewhere in the atomistic region to maintain the appropriate slip step across the atom/continuum interface and into the continuum for the continuum boundary value problem. Within elasticity, the position of this 'ghost' dislocation along the slip plane is arbitrary.

From the above description of the passing of dislocations between atomistic and continuum regions, it is clear that dislocations cannot exist within a distance X from the atom/continuum interface in the range $-\boldsymbol{R}_{A\to C} < \boldsymbol{X} < \boldsymbol{R}_{C\to A}$. Accuracy of the CADD method thus requires that (i) the Peach–Koehler force on a dislocation, whether atomistic or continuum, at the point of passing (i.e. either $\boldsymbol{X} = \boldsymbol{R}_{A\to C}; \boldsymbol{X} = \boldsymbol{R}_{C\to A}$) must be accurately computed and (ii) the equilibrium position of a dislocation should not be in the range $-R_{A\to C} < x < R_{C\to A}$. Both accuracy and computational efficiency of the coupled method dictate that $R_{A\to C}$, $R_{C\to A}$ be as small as possible without spurious forces.

3. Dislocation forces near an atomistic/continuum interface

3.1. Origin of spurious forces

A typical geometry for an atomistic region embedded in a surrounding continuum region, and with a single dislocation dipole, is shown in figure 2(*a*). CADD as well as other coupling methodologies assume linear elasticity in the entire continuum region and implicitly in the atomistic region near the atomistic/continuum interface. The core regions of real dislocations are inherently non-linear and hence the assumption of linearity is violated when dislocations come close to the interface. The linearity/non-linearity mismatch produces spurious forces on the dislocations, as follows.

First, consider the case that is general to atomistic/coupled methods of many types, wherein a dislocation is nucleated and contained within the atomistic region. In the absence of any continuum dislocations, there is no $\tilde{\boldsymbol{u}}$ field. The interface atoms, possibly in the region of non-linear response, provide a displacement boundary condition for the linearly elastic FEM calculation of the total displacement field, which is just the $\hat{\boldsymbol{u}}$ field. The pad atom displacements are thus obtained from the linear $\hat{\boldsymbol{u}}$ field, which is not the true non-linear atomic displacement field. The real atoms then respond to the incorrect pad atom positions, causing spurious forces in the system.

Next, consider the case particular to CADD wherein a discrete dislocation in the continuum is advancing toward the atomistic region (figure 2(*b*)). The core structure described by the continuum linear elastic dislocation field $\tilde{\boldsymbol{u}}$ dictates the positions of the pad atoms, which are not those of a proper atomistic dislocation. The real atoms, possibly moving within the regime of non-linear deformations, then experience incorrect forces due to the imperfect pad atom positions, and move accordingly. The real interface atoms, in incorrect positions, then provide a boundary condition for the continuum elastic FEM solution for the $\hat{\boldsymbol{u}}$ field, which yields new nodal positions and hence new pad atom positions through the $\hat{\boldsymbol{u}}$ field, which again are not the positions the pad atoms would have in a fully atomistic simulation. This process is iterated until convergence is attained but during the entire iteration process a mismatch continually exists between a linear continuum field with a linear $\tilde{\boldsymbol{u}}$ and a non-linear atomistic region. The

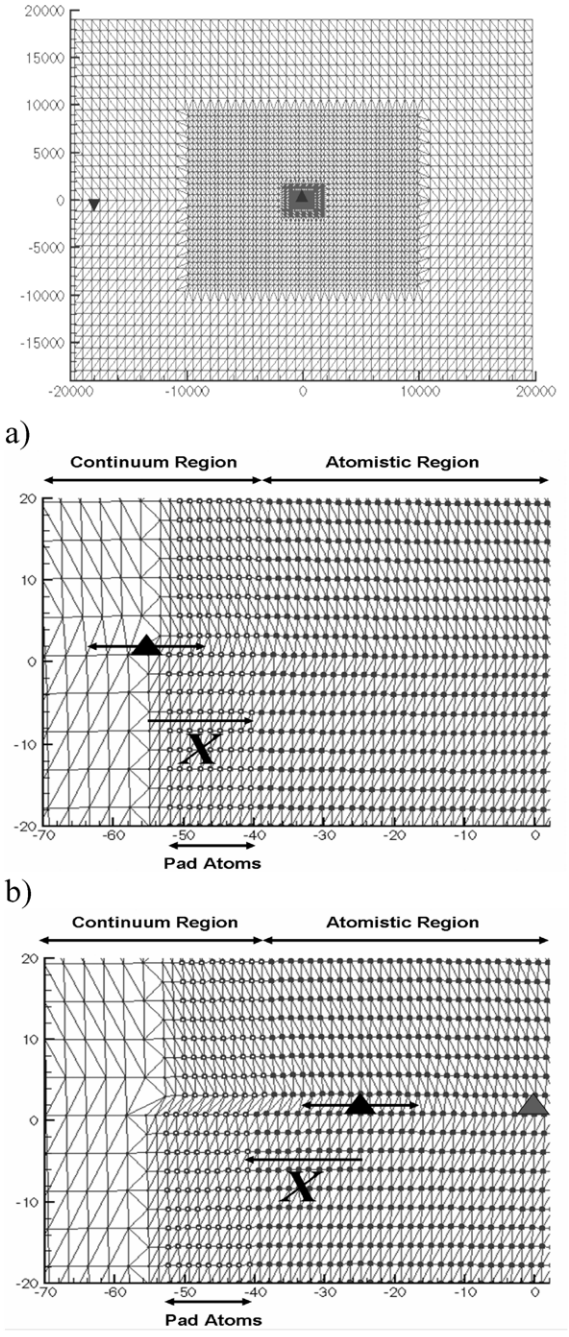

Figure 2. Formulation of the CADD model. (*a*) Full model, with a dislocation dipole as indicated by opposite black triangles; (*b*) close-up with one dislocation in the continuum region at a distance ***X*** from the atom/continuum interface; (*c*) close-up with one dislocation in the atomistic region at a distance ***X*** from interface. Atoms inside the continuum mesh region indicate pad atoms. Partial width spacing of full dislocations is denoted by the double arrowed line; the 'ghost' discrete dislocation (see text) is specified by the grey triangle. All scales are in Angstroms, and the meshing within the atomistic region is for ease of visualization and does not influence the atomic force calculations.

converged displacement and stress fields are thus not exactly those of the full atomistic problem and the Peach–Koehler force on the continuum dislocation is not correct. The degree of error depends on the extent of non-linearity in and around the dislocation core.

Finally, consider the same discrete dislocation being passed into the atomistic region (figure 2(*c*)). As previously mentioned, a 'ghost' discrete dislocation described by the linear elastic $\tilde{\boldsymbol{u}}$ field is necessary to maintain the proper slip across the continuum region. The pad atoms displace according to this continuum ghost dislocation field, and this information is conveyed to the real atoms, which respond to the inaccurate field. The interface atoms then provide an inaccurate boundary condition for the continuum $\hat{\boldsymbol{u}}$ field, and the subsequent superposition with the $\tilde{\boldsymbol{u}}$ field leads to incorrect pad atom positions. Again, the final configuration will give spurious forces on the system due to nonlinearity in the atomic response.

In all cases above, the magnitude of the errors depends on the extent of non-linearity that the atoms would have in a full atomistic system. Since the non-linearity is predominantly in the dislocation core, the errors depend on how close the dislocation core is to the atom/continuum interface. It is important to note that dislocation core splitting into partial dislocations is common in FCC materials and needs to be addressed in the modelling formulation. The leading partial is then closer to the atomistic/continuum interface than the centre of the full dislocation, increasing the distance over which non-linear effects play a role.

3.2. Forces on a continuum dislocation near the interface

The spurious forces on dislocations near the atomistic/continuum interface are now quantified using a model CADD problem. The model consists of an 80 Å by 80 Å atomistic region surrounded by a continuum region of size 38 000 Å by 38 000 Å (figure 2(*a*)). The material used is FCC aluminium, as described by the Ercolessi–Adams EAM potential [17] and the cubic elastic constants. Plane strain conditions are assumed in the through-thickness direction. For the both edge and screw dislocations, the simulation cell has top and bottom surfaces with (111) orientation. The lateral surfaces have $(\bar{1}10)$ orientation for the edge and $(11\bar{2})$ orientation for the screw, while the out-of-plane normal is $(11\bar{2})$ and $(1\bar{1}0)$ for the edge and screw, respectively. A discrete dislocation is placed in the continuum at a distance X away from an atomistic/continuum interface along a slip plane (figure 2(*b*)). An equal and opposite dislocation is placed near the outer boundary of the model, thus conserving mass by introducing a dipole. Both discrete dislocations are held fixed while the atomistic and continuum regions relax to equilibrium. Since the spurious forces are due to non-linear interactions, it is expected that these forces will also be a function of the applied load. Appropriate shear displacements are thus applied on the outer FEM boundary if resolved shear stresses are desired; the only other loads are from the discrete dislocation interactions and their image forces, both of which are negligible because the two dislocations are far apart and the model size is large. Therefore, the resolved shear stress acting on the discrete dislocation near the atomistic/continuum interface should be the applied value. The actual resolved shear stress on the dislocation minus the applied value is then used as a measure of the spurious P–K force induced by the interaction with the atomistic/continuum interface.

It is common in the discrete dislocation methodology to describe the analytic dislocation fields $\tilde{\boldsymbol{u}}$ and $\tilde{\sigma}$ by the isotropic elastic Volterra solution [15, 18–20]. Past CADD studies have used this assumption while maintaining fully anisotropic elasticity in computing the corrective $\hat{\boldsymbol{u}}$ fields, which is one possible source of inaccuracy. We have implemented here fully anisotropic $\tilde{\boldsymbol{u}}$ and $\tilde{\sigma}$ fields in CADD using classical sextet anisotropic elasticity theory [16], so that the discrete dislocations generate fields with orientational dependence. This improves the accuracy of the method, but the non-linearity from dislocation core structures is still not

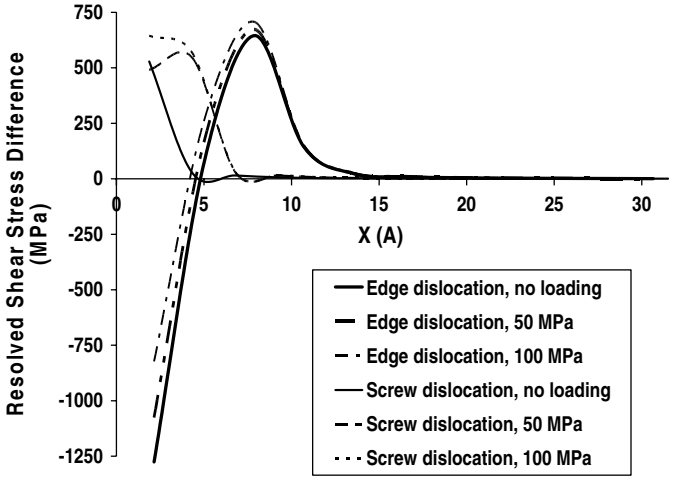

Figure 3. Resolved shear stress difference (measured minus applied) versus distance of a continuum dislocation from the atomistic/continuum interface, for several values of applied loading and for both edge and screw dislocations. The screw dislocation is strongly attracted towards the interface while the edge is strongly attracted and then strongly repelled, with a point of entrapment.

captured by any elastic solution and so spurious effects will be generated for both isotropic and anisotropic models. All results shown here employ anisotropic elasticity.

Figures 3(*a*) and (*b*) show the computed resolved shear stress as a function of distance from the centre of the dislocation to the atom/continuum interface, on edge and screw dislocations, respectively, for several values of applied field and using the anisotropic elastic representations of the $\tilde{\boldsymbol{u}}$ fields. In all cases, there are very large errors in the resolved shear stress (reaching 500–700 MPa) when a discrete dislocation approaches the atomistic/continuum interface, with positive values indicating attraction towards the interface. Stresses this large will definitely disrupt dislocation interaction phenomenon, resulting in dislocation configurations and applied stresses that can either falsely cause or inhibit reactions (e.g. dislocation nucleation, dislocation transmission through grain boundaries, crack growth) in the atomistic region. Moreover, for the edge dislocation the force changes sign and becomes repulsive; there is thus a point of zero force where the edge dislocation is trapped near but not at the interface. Therefore, dislocations should be restricted from entering a region that results in these high values of stress.

For the edge dislocation, various loading conditions do not significantly affect the spurious force on the dislocation. Loading on the screw dislocation leads to increased errors, effectively shifting the zero-load curve by one atomic lattice spacing further from the interface, but the maximum attractive stress and overall shape of the curve are basically the same. The errors are greater, and exist over a larger spatial range, for the edge as compared with the screw dislocation. One reason for the larger effects for the edge relative to the screw is the difference in the core width. For FCC EAM aluminium, full dislocations split into, roughly, leading and lagging partial dislocations with spacings of 14.25 Å and 8.24 Å for the edge and screw, respectively. Thus, the leading partial core will be at the atom/continuum interface when the full dislocation centre is at 7.125 Å for the edge dislocation and 4.12 Å for the screw dislocation. These distances correspond to those with the peak attractive stresses on the dislocation, indicating that the non-linear effects of the leading partial are attractive to the interface. A distinguishing feature for the edge dislocation is that once the leading partial core is fully within the atomistic region, the stress becomes repulsive.

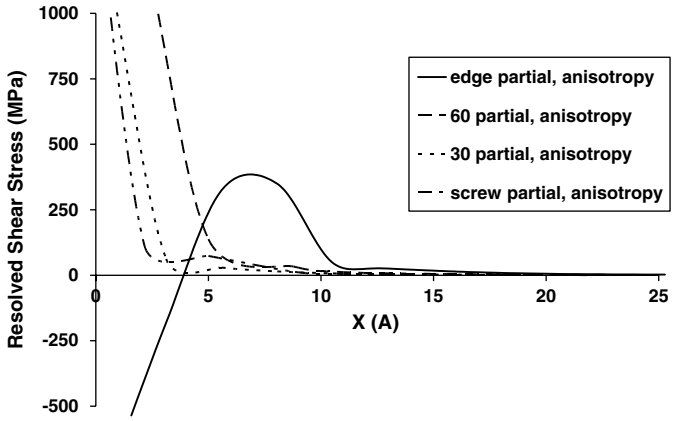

Figure 4. Resolved shear stress, for zero applied load, versus distance of a continuum dislocation from the atomistic/continuum interface, for the 0°, 30°, 60° and edge partial dislocations.

Overall, when using anisotropic elasticity, the distance for passing of dislocations on the continuum side of the interface with errors of 20 MPa or less for all applied loadings considered here is $R_{C\to A} \sim 8$ Å for the screw dislocation and $R_{C\to A} \sim 15$ Å for the edge dislocation. Although not shown, anisotropy provides notably better results than isotropy, particularly at large distances, even when the material studied (FCC aluminium) is not very anisotropic.

In FCC materials, individual Shockley partial dislocations can play an important role in how materials behave. For example, emission of dislocations from grain boundaries in nanocrystalline materials initially produce leading partial dislocations followed by a stacking fault connected to the boundary [22,23]. Dislocation emission from crack tips can also produce twinning from Shockley partials on successive slip planes [24, 25]. Figure 4 thus shows the resolved shear stress versus distance x from the atom/continuum interface for the four types of partial dislocations in FCC Aluminium under zero applied load. The results for the screw, 30°, and 60° partials are similar to the full screw and are strongly attracted to the interface. The edge partial dislocation is similar to the full edge dislocation and will become trapped in the continuum just outside the interface.

3.3. Forces on dislocations in the atomistic region

As argued above, when an atomistic dislocation approaches an atomistic/continuum interface, the dislocation interaction with atoms governed by linear continuum fields leads to spurious forces. Here we deduce the range of such forces, using the model shown in figure 2(*a*) but with the dislocation placed inside the atomistic region at a distance X away from the atomistic/continuum interface, as indicated in figure 2(*c*). In the atomistic region, however, the dislocation cannot be held fixed and the P–K force cannot be directly measured. Thus, indirect approaches are necessary. The displacement field from classical sextet anisotropic theory is initially imposed onto the atomistic region at a chosen dislocation core position and the system is relaxed. Any spurious forces will drive the dislocation to a new equilibrium position. The position of the 'ghost' continuum discrete dislocation, also indicated in figure 2(*c*), plays a role in the accuracy of the solution. Here, two choices for the 'ghost' position are used: (i) at the centre of the atomistic region (40 Å from the interface) and (ii) at the exact location of the atomistic core. Recall that within linear elasticity, the ghost position is arbitrary.

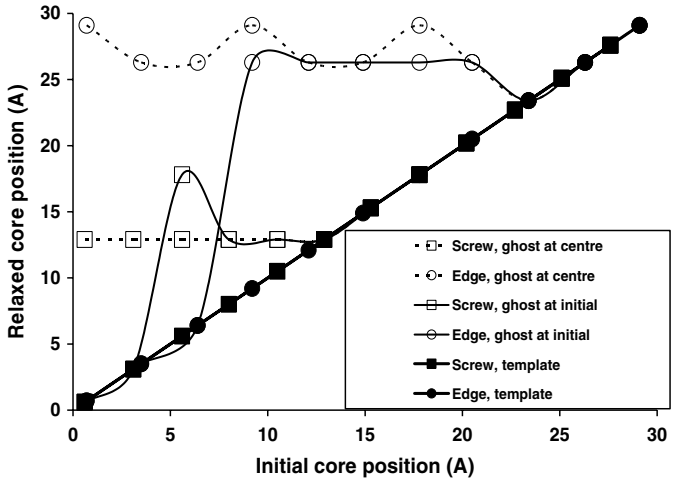

Figure 5. Relaxed dislocation position, relative to the atom/continuum interface, versus initial position for edge and screw dislocations, with the 'ghost' continuum discrete dislocation at the initial position or at the centre of the atomistic cell. Also shown are the results using the proposed template method. Deviations from the straightline of slope unity indicate the existence of spurious forces having moved the dislocation to an incorrect final equilibrium position.

Figure 5 shows the final dislocation core position versus the initial position for screw and edge dislocations, with each of the two choices for the ghost dislocation position. The core position is defined as the centre point between the two partial dislocations and is referenced with respect to the atomistic/continuum interface. In all cases, the dislocation is repelled from the interface. When the ghost screw dislocation is at the centre of the cell, spurious forces repel the true dislocation from the interface to a final relaxed position of 12.9 Å whenever the initial position is closer than 12.9 Å to the interface. For initial positions further than 12.9 Å, the dislocation remains at its initial position, indicating that any spurious forces are smaller than the Peierls barrier of ∼20 MPa [21]. When the ghost edge dislocation is at the centre of the cell, the dislocation is repelled from the interface to a final position that oscillates slightly between 26.3 and 29.1 Å for any initial position closer than 23.4 Å. Since the Peierls barrier for the edge is much smaller than that for the screw [21], and since the core spreading is larger for the edge, it is not surprising that the edge is repelled further from the interface. When the ghost dislocation is placed at the initial position of the true dislocation core, the results are largely similar but at very small distances, <3.1 Å for the screw and <6.3 Å for the edge, the dislocation stays at its initial position, suggesting that the dislocation becomes pinned by the leading partial of the ghost dislocation residing in the continuum pad atom region.

Since the spurious forces on the atomistic dislocations are all repulsive, to further quantify the spurious forces we use the same model but apply a resolved shear stress to the system in an attempt to push the dislocation towards the atomistic/continuum interface. If the dislocation reaches an equilibrium position in the atomistic region, then a spurious repulsive force from the interface exists that is equal and opposite (minus the effects of the Peierls barrier) to the applied stress. Figure 6 shows the dislocation position versus applied shear stress, with the 'ghost' discrete dislocation made to travel with the true atomistic dislocation as it moves during relaxation, which is expected to be the most appropriate strategy for high accuracy. Repulsive stresses for the screw dislocation are greater than the Peierls barrier at distances smaller than about 9.5 A. When the screw reaches 4.9 Å, it remains pinned for applied stress up to 75 MPa.

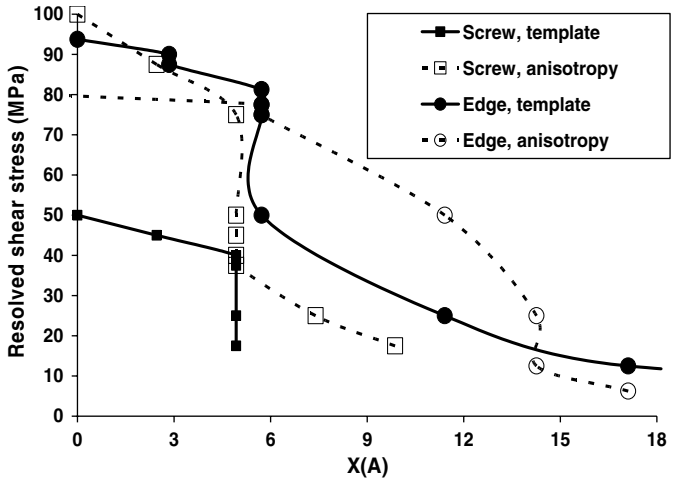

Figure 6. Applied resolved shear stress versus equilibrium dislocation position relative to the atomistic/continuum interface, for edge and screw dislocations. Without spurious forces, all dislocations should be pushed to the interface at $X = 0$. Positions greater than 0 indicate that the interface exerts a spurious repulsive force equal to the applied stress. The new 'template' method shows a significant decrease in the repulsive stress as compared with that obtained from continuum anisotropic elasticity.

At a stress of 100 MPa, the screw can finally move all the way to the interface. The edge dislocation shows repulsive forces at distances smaller than about 18 Å, rising steadily with decreasing distance to about 100 MPa when the dislocation reaches the interface.

The above results indicate that the detection band in the atomistic region must be at $\boldsymbol{R}_{A\to C} \geqslant 13$ Å for screw dislocations and $\boldsymbol{R}_{A\to C} \geqslant 24$ Å for edge dislocations to minimize any spurious forces. For general atom/continuum coupling methods, dislocations closer to the interface will also experience notable spurious forces. In tandem with the results for dislocations in the continuum regime, there is a substantial zone in which dislocations experience spurious forces larger than the Peierls barrier -13 Å $< x < 8$ Å for the screw and -24 Å $< x < 15$ Å for the edge dislocation. Dislocations must thus be passed from one region to another outside of this zone of spurious forces. In the next section, we describe a method to reduce these spurious forces and thus shrink the zone where spurious forces are important.

4. 'Template' method to reduce spurious interface forces

4.1. The 'template' method

Here, we introduce a simple method for modifying the core description of a discrete dislocation so as to capture some of the non-linearity of the dislocation core structure and thus reduce the spurious forces. The key feature of the model is the use of a 'template' of the true positions of the atoms in the dislocation core as a *discrete atomistic* $\tilde{\boldsymbol{u}}$ field whenever the core of the dislocation is near the atom/continuum interface.

To generate a template of the atomistic core that is consistent with a far-field anisotropic linear elasticity solution, we use the standard methods, as follows [13, 14]. A cylindrical atomistic region of radius R_{core} is surrounded by a pad of boundary atoms. An initial continuum dislocation displacement field described by classical sextet anisotropic elasticity is used to displace all interior and boundary atoms. The inner atomistic region is then permitted to relax,

holding the surrounding boundary atoms fixed. The atoms within R_{core} move into relaxed core positions, $\tilde{\boldsymbol{u}}_{\text{relaxed-core}}$, that match up smoothly with the fixed atomic positions given by the anisotropic elasticity solution outside of R_{core}; these displacements are the *discrete* $\tilde{\boldsymbol{u}}$ field because they are the solution for a single dislocation in an effectively infinite anisotropic medium. These relaxed positions are then stored and used in any future CADD model to describe the dislocation core structure as needed. Specifically, when a dislocation comes 'close' to the atom/continuum interface, i.e. within the distance R_{core} on either side of the interface, then the CADD method uses a modified $\tilde{\boldsymbol{u}}$ given by

$$\begin{aligned} \tilde{\boldsymbol{u}} &= \tilde{\boldsymbol{u}}_{\text{relaxed-core}} \qquad x \leqslant R_{\text{core}} \\ \tilde{\boldsymbol{u}} &= \tilde{\boldsymbol{u}}_{\text{anisotropic}} \qquad x > R_{\text{core}}. \end{aligned} \tag{2}$$

When a dislocation is close to the atomistic/continuum interface on the continuum side, the pad atoms will be assigned the non-linear template positions, which are an excellent representation of the stress-free core and provide a better set of positions as boundary conditions for the atomistic region. When a dislocation is in the atomistic region, the 'ghost' dislocation described by the template solution for $\tilde{\boldsymbol{u}}$ will again give the appropriate non-linear displacement field to the pad atoms and generate the appropriate forces on the real atoms. In all cases, then, the real atoms see a more-realistic dislocation core structure in the pad for any dislocations that influence the pad atom positions. The 'template' method gives CADD a feature that is similar to the QC method: as defects approach the atomistic/continuum interface, the 'template' effectively refines the mesh around the dislocation. The full core structure is thus preserved until it is no longer needed.

In the following sections, we re-analyse the same problems studied in section 3 but now using the template solution of equation (2). The extent of the core region, R_{core}, is an adjustable parameter that must be chosen appropriately. If R_{core} is too small, a region of the non-linear core will be represented by the linear solution and this incompatibility can result in spurious stresses. If R_{core} is large, the computational cost increases, although only slightly. We tested two choices of the core radius, 50 and 30 Å, and found much higher spurious stresses using 30 Å. Our results below thus exclusively use R_{core}=50 Å. For FCC Al described by the Ercolessi–Adams EAM potential, 50 Å is equivalent to about 9 times the cut-off radius of the potential. A 50 Å region of non-linearity for the dislocation core is also consistent with the results of Rao *et al* in their study of dislocation core structures using the Lattice Green's Function method [13].

4.2. Results

Figures 7(*a*) and (*b*) show the spurious resolved shear stress (measured minus applied) for edge and screw dislocations, respectively, as a function of distance from the interface on the continuum side as computed using the template method for several applied loads; the previous anisotropic elasticity results are also shown for comparison. For the screw dislocation, the template method works exceptionally well at zero applied load: the error is less than 5 MPa at distances >5 Å from the interface and reaches a maximum value of only 13 MPa at 1.9 Å. Keep in mind that at 1.9 Å, only the lagging partial structure is contained in the pad atom region, so the atomistic region automatically creates the leading partial structure in response to the lagging partial template with almost no distortion. All of the stresses for the screw are well below the Peierls barrier. Under an applied load, the error increases but is negligible at distances >7 Å and reaches 10% of the applied load at 5 Å, increasing smoothly at smaller distances in proportion to the applied load. For the edge dislocation at zero load, the template method also shows improvement over the anisotropic elasticity description with an error of 25 MPa occurring at just 5 Å. Closer to the interface, the template method shows increased stress but

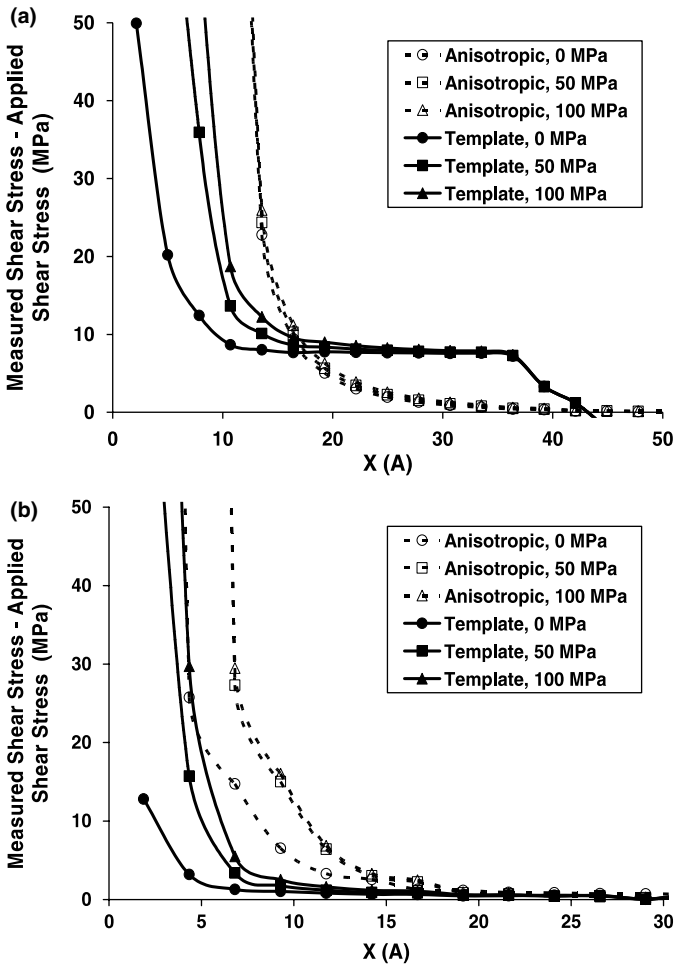

Figure 7. Resolved shear stress difference (measured minus applied) versus distance of a continuum dislocation from the atomistic/continuum interface, for several values of applied loading and for both (*a*) edge and (*b*) screw dislocations. Results from anisotropic elasticity (figure 3) are also shown for comparison (data for $\boldsymbol{X} < 5\boldsymbol{A}$ for the edge not shown, for clarity).

does not change sign and reaches a peak value of only 50 MPa at 1.87 Å. Under applied loads, the spurious stresses start to increase at about 10 Å from the interface. However, at distances from 5 to 50 Å, the template method introduces a small constant error of ∼9 MPa. Although the template $\tilde{\boldsymbol{u}}$ displacement field smoothly matches the continuum anisotropic elasticity solution by construction, there is evidently some small discrepancy in the description. The effect is probably constant with distance because there is always a portion of the outer edge of the cylindrical template impinging on the boundary at some lateral position away from the slip plane of the dislocation.

For dislocations in the atomistic region, we compute the equilibrium position of a dislocation introduced at a particular location in the cases with zero or non-zero applied loading. In using the template method, we place the 'ghost' dislocation at the same position as the initial dislocation. For zero applied load, figure 5 shows that the equilibrium position of the dislocation is exactly that of the initially-placed dislocation for both screw and edge

dislocations. This is to be expected since, for zero applied load, we have used the true atom positions in the pad. We then apply a shear force to drive the dislocation towards the interface and measure the position at which the applied force is balanced by any spurious forces, as shown in figure 6. The screw dislocation moves to within 5 Å at stresses just above the Peierls barrier, indicating no spurious forces up to that point, which is one-half the distance found when using anisotropic elasticity. The screw moves to the interface at a stress of 50 MPa, one-half the value when no template is used. For the edge dislocation, the spurious forces begin at distances of ∼15 Å comparable to those found using anisotropic elasticity, but increase more slowly with distance between 15 and 6 Å. An applied stress of 90 MPa is then needed to move the dislocation to the interface. The results for the edge are thus slightly better than when using anisotropic elasticity.

In all cases, the template method reduces the spurious forces acting on dislocations near the atomistic/continuum interface and renders them less erratic. This is the main result of this paper.

The template method is presently usable for full dislocations but not for partial dislocations. For partial dislocations, we have not yet developed a procedure for extracting the proper core structure. Simply introducing a single partial in an atomistic simulation under zero applying loading is not viable because such a situation is not in equilibrium: the stacking fault energy generates a configurational force on the partial that is unbalanced and so the partial dislocation will move within the computational cell until boundary or interface forces counteract the stacking fault force. Such an 'equilibrium' state is thus associated with the imposition of uncontrolled external forces and does not yield a correct core structure. The partial dislocation can be stabilized by application of a uniform applied load on the computational cell that exactly counteracts the stacking fault force. However, this loading affects the core structure and also generates far-field deformations. Since the core region is non-linear, the applied far-field deformation cannot be subtracted out to give the correct core positions. Different subtraction algorithms were applied in an attempt to obtain errors in the resolved shear stress below those from anisotropic elasticity, but to date these attempts have been unsuccessful. Therefore, we do not yet have a proper template for partial dislocations.

4.3. Implications for detection and passing of dislocations

The new 'template' method allows dislocations to reach closer to the atomistic/continuum interface before significant spurious forces occur, thus allowing for a more-seamless passing of dislocations between the atomistic and continuum domains. Here we address the issue of passing more carefully for each case, in light of the results above.

The results obtained here at zero applied load are most relevant, since they correspond to equilibrium positions for the dislocations. If loads above the Peierls barrier are acting on a dislocation, due to applied loads and interactions with other dislocations or real interfaces, the dislocation is not in equilibrium and thus will move towards equilibrium. The spurious forces shown here under applied loads will influence the *approach* to equilibrium but not necessarily affect the equilibrium position itself. Let us consider each case in turn.

When a screw dislocation approaches the interface from the continuum, the spurious forces are always attractive (figure 7(*b*)). Therefore, the distance $R_{C\to A}$ can essentially be set to zero without influencing the fate of the dislocation, unless the true equilibrium position is very close to the interface. Once the screw dislocation passes into the atomistic region near the interface, the spurious forces are always repulsive and push the dislocation away from the interface (figures 5 and 6). Therefore, the distance $R_{A\to C}$ can essentially be zero. When a screw dislocation in the atomistic region approaches the interface, the spurious forces

are repulsive, and so the dislocation must be passed prior to reaching the interface. Our results indicate $\boldsymbol{R}_{A\to C} = 5$ Å. Once the screw dislocation is passed to the continuum, spurious attractive force exists near the interface. Thus, the dislocation must be passed to a distance $\boldsymbol{R}_{C\to A} = 5$ Å to avoid any spurious effects. Therefore, for screw dislocations approaching from either direction, we can select a minimal region of only 10 Å in width, -5 Å $< \boldsymbol{X} < 5$ Å, with negligible effect of any spurious forces on the dislocation. The action of passing the dislocation abruptly over any distance also causes a perturbation to the system, and so minimizing the passing distance to 10 Å probably gives the best results in speed of convergence as well as accuracy.

When an edge dislocation approaches the interface from the continuum side, the spurious forces are again attractive when the template is used, and thus cause minimal problem with passing. To avoid spurious forces requires passing at a distance $\boldsymbol{R}_{C\to A} = 10$ Å. When the edge dislocation is passed to the atomistic domain, the spurious forces are repulsive and do not hinder the dislocation motion. When an edge dislocation is in the atomistics and approaching the interface the spurious forces are always repulsive. The dislocation must be passed to the continuum at a distance of $\boldsymbol{R}_{A\to C} = 13$ Å if spurious stresses are to be limited to 25 MPa. If the edge dislocation is passed to the continuum near the interface, it is attracted to the interface. It must thus be passed to a distance of $\boldsymbol{R}_{C\to A} = 10$ Å. Therefore, for edge dislocations approaching from either direction, we can select a minimal region of only 23 Å in width, -13 Å $< \boldsymbol{X} < 10$ Å, with negligible effect of any spurious forces on the dislocation.

The results in figures 5 and 6 show that it is necessary, for accurate results, to have the ghost discrete dislocation position track the true position of the atomistic dislocation core. To properly place the ghost discrete dislocation thus still requires the detection of the true dislocation core within the atomistic region even outside of the passing distance $\boldsymbol{R}_{A\to C}$ specified above. Thus, the concept of a detection band must be broadened and separated from the concept of the passing distance. The CADD method must be modified by using a true annular band of 'detection band' elements, rather than just a band of width equal to one atomic planar spacing at a distance from the interface. The annular band of elements extends from a distance R_{DB} that denotes the inner edge of the detection band to a distance $\boldsymbol{R}_{A\to C}$ from the atom/continuum interface, as shown schematically in figure 8. Passing of the dislocation can be done when the atomistic dislocation reaches the independent position $R_{A\to C}$, determined from studies such as those in the previous sections. Thus, a detection band exists as a monitoring device for all dislocations near the atom/continuum interface, but dislocation motion is not influenced in any way until a dislocation reaches the passing distance $\boldsymbol{R}_{A\to C}$.

To be more specific, when a dislocation generated in the atomistic region moves towards the atom/continuum interface, it enters the detection band region at $\boldsymbol{R}_{\mathrm{DB}}$, where its Burger's vector and slip plane are identified (figure 8(*a*)). A 'ghost' discrete dislocation having the same characteristics is then introduced at the same position. As the atomistic dislocation core moves closer to the interface under the action of other forces, the core position is continuously detected within the detection band elements and this information is used to update the positions of the 'ghost' discrete dislocation. This process minimizes any spurious forces. When the atomistic dislocation reaches the distance $\boldsymbol{R}_{A\to C}$ (figure 8(*b*)), the atomistic dislocation is passed to the continuum as a real discrete dislocation. Operationally, at this point the 'ghost' dislocation moves into the continuum domain and becomes a real dislocation and the atomistic dislocation is annihilated by *subtracting* a template $\tilde{\boldsymbol{u}}$ field at the position of the atomistic core at the instant of passing. Furthermore, a continuum dislocation can be passed into the atomistic region to a position just inside $R_{A\to C}$, where it automatically becomes a 'ghost' dislocation. The detection band near the interface then continues to detect the atomistic core of the dislocation until it

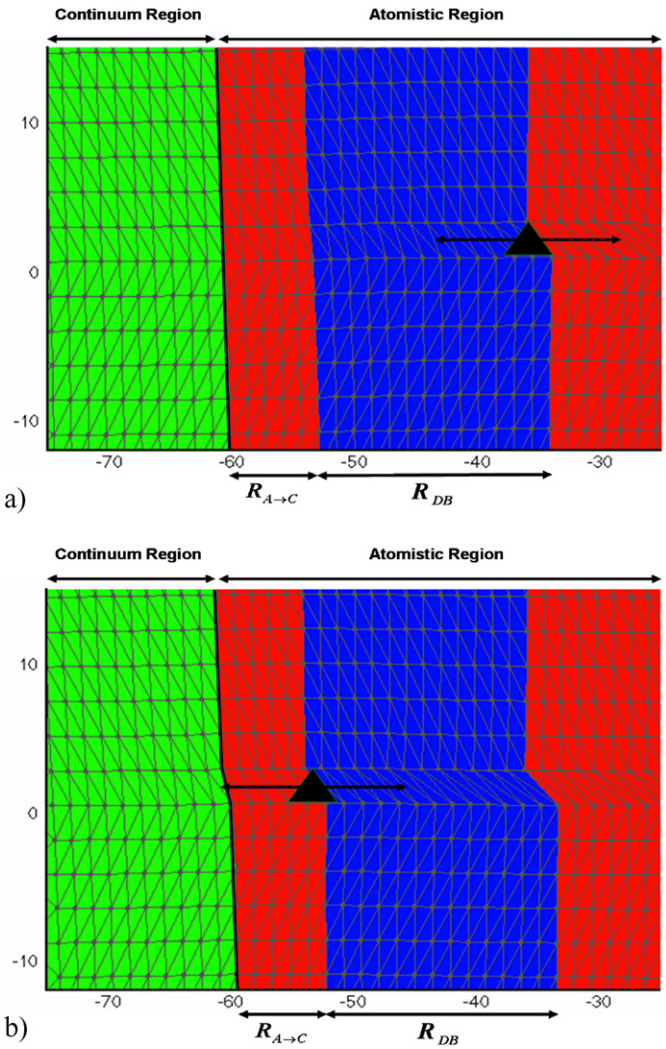

Figure 8. Schematic of modified dislocation detection band concept. Dark (blue) elements indicate the detection band strip R_{DB} residing in the atomistic region. An atomistic dislocation core within the detection band region carries a 'ghost' discrete dislocation (black triangle) moving with the true core; atomistic dislocation is passed to the continuum when it reaches the distance $R_{A\to C}$. Elements in the atomistic region do not influence the atomic force calculations.

leaves the detection band and moves into the remainder of the atomistic region or until it is pushed back into the continuum by other forces. If the dislocation core moves into the inner atomistic region, the 'ghost' discrete dislocation can then safely be placed at any convenient location away from the interface along the slip plane of the dislocation without introducing any spurious forces.

The above new detection band concept along with the template method thus minimizes the spurious forces and hence minimizes the region $-\boldsymbol{R}_{A\to C} < \boldsymbol{X} < \boldsymbol{R}_{C\to A}$ within which dislocations are not permitted. The detection band and template method together can also be employed in other atom/continuum coupling models to minimize the interactions of atomistic dislocations with the atom/continuum interface and thus provide the same advantages of

increased accuracy or use of smaller atomistic domains that the method confers on the CADD model.

5. Summary

We have shown that spurious forces can arise due to interactions of dislocations with an artificial atomistic/continuum interface and have evaluated all of the various cases within the context of the CADD model. The spurious forces, which can attract, repel or trap dislocations near the interface, arise due to the non-linear/linear mismatch in atomistic and continuum descriptions of both the dislocation cores and the material response. We have quantified the spurious forces for various dislocations in Al within an anisotropic elasticity treatment for the continuum. To avoid spurious forces above 20 MPa for any applied load level, dislocations must be excluded from the region $-13\,\text{Å} < \boldsymbol{X} < 10\,\text{Å}$ for edge dislocations and $-15\,\text{Å} < \boldsymbol{X} < 10\,\text{Å}$ for screw dislocations, where the atom/continuum interface is at $\boldsymbol{X} = 0$. Most importantly, we have introduced the 'template' method as a means of reducing these spurious forces and making the forces always attractive to the interface in the continuum region and repulsive in the atomistic region. The template method uses the true atomistic core displacement fields within a radius R_{core} and thus permits conveyance of the proper non-linear displacement field to the pad atoms that serve to couple the atomistic and continuum regions. Quantitatively, the template method shrinks the excluded region for dislocations to $-13\,\text{Å} < \boldsymbol{X} < 10\,\text{Å}$ for edge dislocations and $-5\,\text{Å} < \boldsymbol{X} < 5\,\text{Å}$ for screw dislocations in aluminium, nearly eliminating any error for atomistic dislocations approaching the atom/continuum interface. This latter achievement permits the CADD method to pass dislocations over very small distances, only 10 Å, thus approaching a completely seamless atom/continuum multiscale method. However, dislocations in the atomistic region must still be *detected* as distinct entities at distances of ∼20 Å from the interface.

Use of the template method proposed here within the CADD framework makes the CADD method as close to an artefact-free multiscale model as we believe possible. Additional work remains to handle properly fully dissociated partial dislocations and to examine the accuracy of the template method in finite-T molecular dynamics version of CADD [26].

Finally, the spurious forces that arise due to interaction of a dislocation core with the atomistic/continuum interface are a harbinger of the difficulties that will arise in developing fully-3d CADD-type models. When dislocation loops exist that have segments in both atomistic and continuum regions, a region of the core of the loop will intersect that atom/continuum boundary. The non-linearity of the core displacements will be imposed directly on the interface, with ensuing spurious forces that will distort the dislocation loop shape and modify its motion. However, the use of a discrete atomistic template, such as that proposed here, for segments of dislocations at the interface may minimize such spurious forces and provide a viable method. One certain difficulty is the need to address the variation in possible dislocation characters for those segments traversing the atom/continuum interface. These challenging issues remain to be tackled.

Acknowledgments

This work was supported by a grant from the US Air Force Office of Scientific Research through the MURI program 'Virtual Design and Testing of Materials: a Multiscale Approach' and by the General Motors/Brown Collaborative Research Laboratory for Computational Materials Science.

References

[1] Rudd R E and Broughton J Q 2000 Concurrent coupling of length scales in solid state systems *Phys. Status Solidi* b **217** 251–91

[2] Kohlhoff S, Gumbsch P and Fischmeister H F 1991 Crack propagation in BCC crystals studied with a combined finite-element and atomistic model *Phil. Mag.* A **64** 851–78

[3] Rudd R E and Broughton J Q 1998 Coarse-grained molecular dynamics and the atomic limit of finite elements *Phys. Rev.* B **85** R5893–6

[4] Wei Cai, M de Koning, Bulatov V V and Yip S 2000 Minimizing boundary reflections in coupled-domain simulations *Phys. Rev. Lett* **85** 3213–6

[5] Shenoy V B, Miller R, Tadmor E B, Rodney D, Phillips R and Ortiz M 1999 An adaptive finite element approach to atomic-scale mechanics—the quasicontinuum approach *J. Mech. Phys. Solids* **47** 611–42

[6] Shenoy V B, Miller R, Tadmor E B, Phillips R and Ortiz M 1998 Quasicontinuum models of interfacial structure and deformation *Phys. Rev. Lett.* **80** 742–5

[7] Miller R E and Tadmor E B 2002 The quasicontinuum method: overview, applications and current directions *J. Comput.-Aided Mater. Des.* **9** 203–39

[8] Shilkrot L E, Curtin W A and Miller R E 2002 A coupled atomistic/continuum model of defects in solids *J. Mech. Phys. Solids* **50** 2085–106

[9] Shilkrot L E, Miller R E and Curtin W A 2002 Coupled atomistic and discrete dislocation plasticity *Phys. Rev. Lett.* **89** 025501-1–025501-4

[10] Miller R E, Shilkrot L E and Curtin W A A Coupled atomistics and discrete dislocation plasticity simulation of nanoindentation into single crystal thin films *Acta Mater.* **52** 271–84

[11] Shilkrot L E, Miller R E and Curtin W A 2004 Multiscale plasticity modeling: coupled atomistics and discrete dislocation mechanics *J. Mech. Phys. Solids* **52** 755–87

[12] Curtin W A and Miller R E 2003 Atomistic/continuum coupling in computational material science *Modelling Simul. Mater. Sci. Eng.* **11** R33–R68

[13] Rao S, Hernandez C, Simmons J P, Parthasarathy T A and Woodward, C 1998 Green's function boundary conditions in two-dimensional and three-dimensional atomistic simulations of dislocations *Phil. Mag.* A **77** 231–56

[14] Woodward C and Rao S I 2004 *Ab-initio* simulation of $(a/2) < 110$ screw dislocations in γ-TiAl *Phil. Mag* **21** 401–13

[15] Van der Giessen E and Needleman A 1995 Discrete dislocation plasticity: a simple planar model *Modelling Simul. Mater. Sci. Eng.* **3** 689–735

[16] Hirth J P and Lothe J 1982 *Theory of Dislocations* 2nd edn (New York: Wiley)

[17] Ercolessi F and Adams J B 1994 Interatomic potentials from first-principles calculations: the force-matching method *Europhys. Lett.* **26** 583–97

[18] Kubin L and Canova G 1992 The modeling of dislocation patterns *Scr. Metall. Mater.* **27** 957–62

[19] Zbib H M, Rhee M and Hirth J P 1998 On plastic deformation and the dynamics of 3D dislocations *Int. J. Mech. Sci.* **40** 113–27

[20] Schwarz K W 1997 Interaction of dislocations on crossed glide planes in a strained epitaxial layer *Phys. Rev. Lett.* **78** 4785–8

[21] Olmsted D L, Hector L G, Curtin W A and Clifton R J 2005 Atomistic simulations of dislocation mobility in Al, Ni and Al/Mg alloys *Modelling Simul. Mater. Sci. Eng.* **13** 371–88

[22] Van Swygenhoven H, Caro A and Farkas D 2001 Grain boundary structure and its influence on plastic deformation of polycrystalline FCC metals at the nanoscale: a molecular dynamics study *Scr. Mater.* **44** 1513–16

[23] Yamakov V, Wolf D, Phillpot S R, Mukherjee A K and Gleiter H 2002 Dislocation processes in the deformation of nanocrystalline aluminum by molecular-dynamics simulation *Nature Mater.* **1** 45–8

[24] Hai S and Tadmor E B 2003 Deformation twinning at aluminum crack tips *Acta Mater.* **51** 117–31

[25] Farkas D 2005 Twinning and recrystallisation as crack tip deformation mechanisms during fracture *Phil. Mag.* **85** 387–97

[26] Qu S, Shastry V, Curtin W A and Miller R E 2005 A finite temperature dynamic coupled atomistic discrete dislocation method *Modelling Simul. Mater. Sci. Eng.* **13** 1101–18